JOURNAL OF CATALYSIS 137, 368–376 (1992)

An FTIR Spectroscopic View of the Initiation of Ethylene Polymerization on Cr/SiO_2 Catalyst

P. ZIELINSKI[1] AND I. G. DALLA LANA

Department of Chemical Engineering, University of Alberta, Edmonton, Alberta, Canada T6G 2G6

Received August 19, 1991; revised March 27, 1992

The onset of polymerization of ethylene on Cr/SiO_2 catalyst activated by high-temperature treatment was studied at room temperature using fast-scanning FTIR spectral measurements. Initial rapid adsorption of molecular ethylene on the pre-activated catalyst preceded the onset of polymerization. A time-delay between adsorption and polymerization was observed. The experimental evidence suggests that initiation of polymerization follows dissociation of ethylene, presumably on two Cr sites. Propagation and other mechanistic steps then follow as suggested earlier.

INTRODUCTION

Views concerning the mechanism of ethylene homopolymerization on a Cr/SiO_2 catalyst remain conflicting despite the commercial significance of this reaction and the amount of related research which has been reported. The initiation step is especially controversial, and McDaniel states (*1*), "the incorporation of the first ethylene is poorly understood, but it is probably different and slower than incorporation of succeeding monomer." Hogan (*2*) proposed polymer growth as shown in Eq. (1):

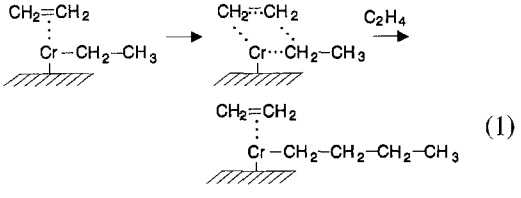

(1)

His view implied that a methyl group terminates each polymer chain but provided no explanation for the origin of the additional hydrogen atom required per chain. McDaniel *et al.* (*3*) considered the possibility of β-elimination of a hydrogen from a chain disengaging from an active site, the hydrogen then transferring to the new chain growing on the site. Silanols have also been proposed as sources of the initial hydrogen atom (*4*, *5*), but McDaniel and Welch (*6*) argue that the polymerization still proceeds rapidly when the silanols are removed.

To avoid the involvement of the controversial hydrogen, other initiation mechanisms have also been proposed. McDaniel summarized a mechanisn, originally proposed by Krauss (*7*) and shown in Eq. (2), in which two ethylenes interact on a single Cr site with an allylic species developing. Other similar approaches have been offered (*8*, *9*); for example, Chiotti *et al.* (*9*) proposed a type of alkyl chain attached to surface chromium atoms from two ends with one end being metallacycle.

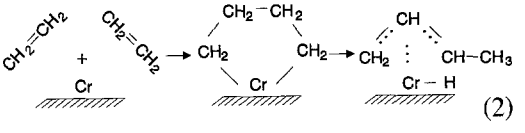

(2)

Earlier, Rebenstorf and Larsson (*10*) proposed, for low-temperature polymerization, a two-chromium atom active site with a $Cr–CH_2–R–CH_2–Cr$ structure (*11*). Whether mono- or dinuclear sites participate in the initiation as well as the nature of

[1] On leave from Technical University of Lodz, Poland.

0021-9517/92 $5.00

the active Cr site are issues that also have been debated, starting from early arguments about stabilization of active surface species in chromate or dichromate forms (*1*). From studies of CO adsorption at low temperatures, Rebenstorf (*12, 13*) suggested that the dinuclear site was the only active one for the polymerization of ethylene at relatively low temperatures.

Recent studies examining the polymerization mechanism have focused upon IR-based evidence, generated during the early stages of polymerization (*4, 9, 14, 15*). The work reported here is a continuation of earlier work (*4*) but utilizes a modern FTIR spectrometer to examine the reaction origins during the earliest seconds of polymerization.

EXPERIMENTAL DETAILS

Materials

The catalysts were prepared by impregnating silica (Cab-O-Sil M-5) using aqueous solutions of CrO_3 (obtained from Fisher), followed by drying at 105°C and calcination at 550°C for 16 h. The calculated total Cr content was nominally 0.5 wt% although atomic absorption analysis of the catalyst sample used to obtain the ethylene adsorption isotherm was 0.4 ± 0.01%. For FTIR transmission measurements, the finely divided catalyst powder was compressed into thin wafers (12 to 30 mg/cm^2).

Procedures

The catalyst wafers were placed in a modified Kiselev type of transmission ir-cell, activated in place by heating in dry oxygen for 2 h at 750°C, followed by high-vacuum treatment for 30 h. This type of activation treatment was developed earlier (*16*). Lunsford and co-workers (*17–19*) claimed that high-temperature evacuation improved the activation of Cr(II) and Cr(III) species. In our work, it was essential for reproducibility of kinetics behaviour at low pressures of ethylene and at reaction initiation conditions to avoid both the influences of residual surface species and possible variations in numbers of reduced Cr sites produced during normal use of CO or C_2H_4 as reducing agents. For example, we observed that after reduction with CO and evacuation at 350°C, in one case, polymerization was only initiated at a minimum ethylene pressure of about 105 Pa. At a sufficiently high pressure of ethylene for polymerization, both thermal and CO activations were equally effective. To obtain kinetics measurements free of factors attributable to differences between catalyst wafers, the wafer was subjected to repeated oxidation–activation cycles (usually three to five were required) until the catalytic activity stabilized. Only then were the initial rates of polymerization measured for different initial ethylene pressures.

The modified Kiselev-type cell (*20*) was used as a batch reactor to study the polymerization of ethylene at room temperature and at ethylene pressures ranging from 1.0 to 5300 Pa. In most runs, 105 Pa ethylene pressure was used as the standard condition unless noted otherwise. By lowering the reaction rate through operation at room temperature and low ethylene pressure, heating of the catalyst wafer above room temperature was minimized. The FTIR spectral scans were obtained using a Nicolet Model 740 spectrometer, operated at up to 9.142 scans per second with a resolution of 4 cm^{-1}. Up to 1280 such spectral scans could be completed and stored in the computer memory at one time. A 32-scan averaging procedure was standardly employed to minimize noise in the spectral data.

RESULTS

FTIR Spectra

The FTIR spectral data used in this study were recorded either as individual scans every 0.1094 s or as an average of a number of consecutive scans to smooth the data for transient conditions. To smooth steady-state spectra, averaging of a large number of spectral scans was possible. Even though the noise level of the FTIR spectrometer in single scans ranged about ±0.005 absorbance units (see solid curve in Fig. 1),

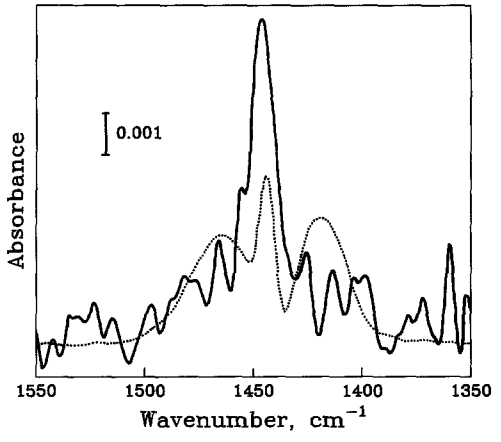

FIG. 1. Typical FTIR spectral scans: (———) Single scan of 0.11 s (polymerization after 2 s with 106 Pa ethylene); (···) Average of 32 scans (1.33 kPa gaseous ethylene).

continuous monitoring of specific IR band absorbances indicated systematic trends. Since the interpretations of such spectral changes were relative, and thus largely qualitative, a more detailed analysis of error was not necessary. The broken line of Fig. 1 shows an averaged steady-state spectral scan for gaseous ethylene.

Figure 2 shows the absorbances of four IR absorption bands plotted as a function of consecutive scans (10 scans per 1.094 s), starting at scan 160 (background) when ethylene was injected into the cell. Absorbances are plotted for individual scans for the initial approximately 2 s; thereafter, the average of each 20 subsequent consecutive absorbances is plotted at the center of the interval. The particular bands being monitored are listed below:

cm^{-1}	Vibration/functional group
1446	$=CH_2$ bending (presumably adsorbed ethylene)
1472	$-CH_2-$ bending (polyethylene) plus a contribution from adsorbed ethylene
2850	$-CH_2-$ symmetric stretching (polyethylene)
2920	$-CH_2-$ asymmetric stretching (polyethylene)

The basis for the 1446 and 1472 cm^{-1} band assignments is discussed shortly.

While the initial single-scan absorbance values for the 1472-cm^{-1} band are noisy, the trend of both 1446- and 1472-cm^{-1} plots to the origin at 160 scans (when ethylene is introduced) is unmistakable. The nonlinear initial trend of the 1472-cm^{-1} plot differs from the complete linearity of the 2850- and 2920-cm^{-1} bands. The shape of the initial curved section for the 1446-cm^{-1} plot resembles adsorptive uptake of ethylene on the catalyst and, in parallel, the 1472-cm^{-1} plot may also be so interpreted. Evacuation of the IR cell after 2 s reduces the ab-

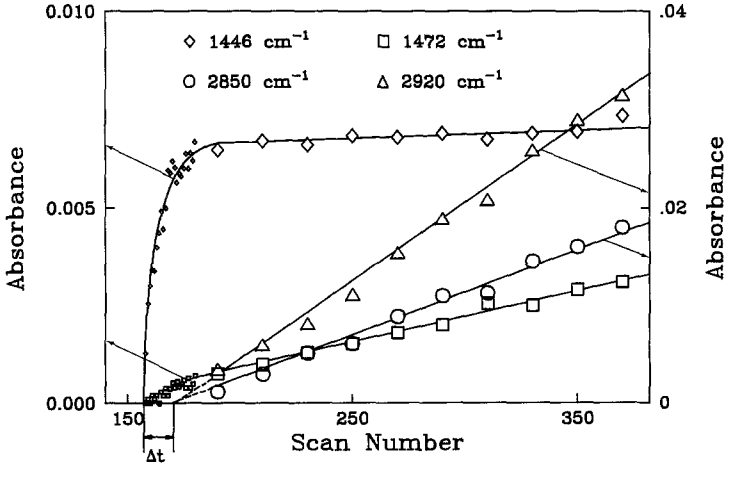

FIG. 2. Adsorption and polymerization of ethylene monitored using FTIR spectroscopy.

sorbance of the 1446-cm^{-1} and the 1472-cm^{-1} bands to zero, indicative of reversible adsorption of ethylene for the 1446-cm^{-1} band. Evacuation well beyond 2 s still decreases the absorbances of both bands but now to finite residual values. For the 1472-cm^{-1} band, the drop is like that observed earlier at 2 s. For the 1446-cm^{-1} band, the drop is roughly 80% of that observed after 2 s indicating that some of the adsorbed ethylene is being retained (shown in Fig. 4). The differences before and after evacuation at 2 s and beyond 2 s change with time, suggesting that some ethylene is being increasingly retained within the polymer/catalyst mass (solubility of ethylene in polymer?) or that the population of adsorbing active Cr sites for ethylene is being lowered because they are increasingly being occupied by the initiation of polymer chains on these active Cr sites.

The smoothed spectrum of gaseous ethylene in Fig. 1 shows a central strong band at 1446 cm^{-1} separating two wing-like bands at 1472 and about 1420 cm^{-1}.

The slight increase in absorbance with time of the 1446-cm^{-1} band can be attributed to overlap from the corresponding larger increases in absorbance of the 1472-cm^{-1} band with polymerization. These two effects are visible in Fig. 3, which shows averaged spectra at scans (times) of 190, 500, and 800 (20.7, 54.7, and 87.5 s). After evacuation at 1310 scans (143.3 s), the decrease in curve (d) of Fig. 3 shows that much of the 1446-cm^{-1} band intensity is related to the presence of ethylene, but a small residual peak remains (retained ethylene after evacuation as per Fig. 2). On the other hand, curve d is inconclusive concerning the 1472-cm^{-1} band because polymerization continued between the 800 and 1310 scans. The 1472-cm^{-1} band is clearly related to the polymerization of ethylene but, as Fig. 3 shows, the 1446-cm^{-1} band may also overlap onto the 1472-cm^{-1} band plot, and this could account for the fact that the 1472-cm^{-1} band does not extrapolate to an origin common with the other two polymer-related bands at 2850 and 2920 cm^{-1} (see Fig. 2).

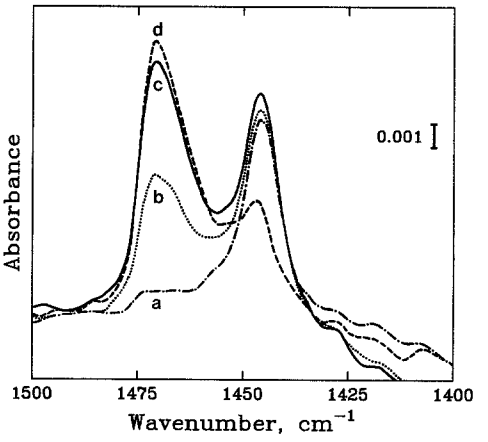

FIG. 3. Changes in 1446- and 1472-cm^{-1} bands with polymerization (averages of 20 scans): (a) after 190 scans; (b) after 500 scans; (c) after 800 scans; (d) after 1310 scans but preceded by evacuation at about 900 scans.

Figure 4 shows clearly that evacuation (removal of ethylene) at about 880 scans decreases the absorbance of both of these bands but no longer to zero absorbance. The 1446-cm^{-1} band continues to decrease very slowly with evacuation between scans 880 and 1310; hence, desorption of ethylene becomes more difficult with increasing mass of polymer in the catalyst pores. The absence of further decreases in the 1472-cm^{-1} band with evacuation also supports the view that overlap from the 1446-cm^{-1} band is involved. In Fig. 2, the plots of the two strongest absorption bands, 2850- and 2920-cm^{-1}, are linear and extrapolate to a time, $\Delta(t)$, after ethylene was injected into the cell. The 1446- and 1472-cm^{-1} plots differed from those of the previous two bands in that they commenced with the introduction of ethylene. Figure 1 also showed a shift of 2 cm^{-1} between the 1446-cm^{-1} band of ethylene adsorbed on active catalyst and the corresponding band for gaseous ethylene. This shift was repeatedly observed. Surprisingly, this shift is downwards towards a higher frequency.

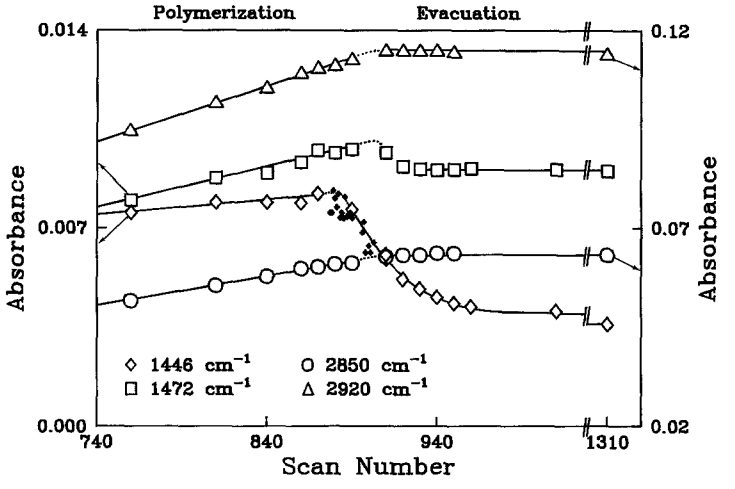

FIG. 4. FTIR spectral changes with time after evacuation of IR cell following 80 s polymerization.

Assuming that polymerization commences $\Delta(t)$ seconds after the introduction of ethylene, the absorbance values preceding the start of polymerization in Fig. 2 should relate to the adsorption character of ethylene and be influenced by the initial pressure of the ethylene introduced. On this basis, similar plots were obtained at several initial ethylene pressures using the same catalyst wafer. The catalyst was regenerated by oxidation and activated before each of these experiments. The 1446-cm^{-1} absorbances corresponding to the intercept from the extrapolation of the linear section to the time, $\Delta(t)$, the start of polymerization, are plotted versus the initial ethylene pressure in Fig. 5. The corresponding absorbances of gaseous ethylene in the empty cell and with inactive oxidized catalyst in the cell are also shown. The data show that ethylene did not adsorb detectably on the oxidized catalyst. By subtracting the latter absorbances from those of the extrapolated previous values, one obtains the type of "isotherm" shown by the solid line in Fig. 5.

While performing the experiments involving early polymerization at different initial pressures of ethylene, the absorbances of not only the 1446-band but also the bands at 2920-, 2850-, and 1472-cm^{-1} were observed to increase with time. The time delay, $\Delta(t)$, also changed with ethylene initial pressure.

For the initial 10 s of reaction, Fig. 6 plots the slope of the 2920-cm^{-1} absorbance versus time curve (as per Fig. 2), which is proportional to the initial rate of polymerization, for various initial ethylene pressures.

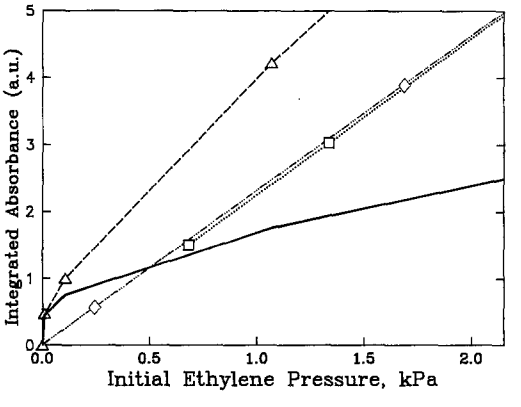

FIG. 5. Adsorption of ethylene on activated Cr/SiO_2 (1446-cm^{-1} absorbance) as a function of initial pressure of ethylene: (◇) IR cell without catalyst, or IR cell with oxidized (inactive) catalyst; (△) IR cell with active catalyst and ethylene; (———) Adsorption behaviour of ethylene (using absorbance to denote surface concentration of ethylene); difference of previous two spectra.

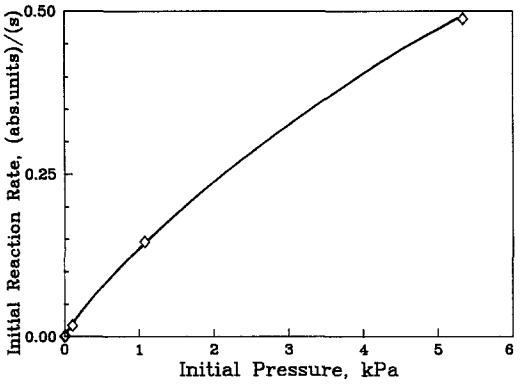

FIG. 6. Dependency of initial reaction rate (based on 1920-cm^{-1} band) upon initial ethylene pressure (at room temperature).

The same catalyst wafer was used to obtain this set of rates. The slight curvature indicates that the rate function is about 0.8 order in ethylene pressure. The IR cell was kept at room temperature, but the catalyst wafer was likely about 10°C higher from heating by the IR beam.

Figure 7 shows that the induction period before polymerization commenced, $\Delta(t)$, is inversely proportional to the square root of the initial ethylene pressure over the same range of initial pressures of ethylene used in Fig. 6. At higher initial pressures, the plot suggests that this simple proportionality may no longer be valid. Experiments in which a step increase in ethylene pressure was made after polymerization had started showed no significant induction period. The induction period was only observed after ethylene contacted freshly activated catalyst.

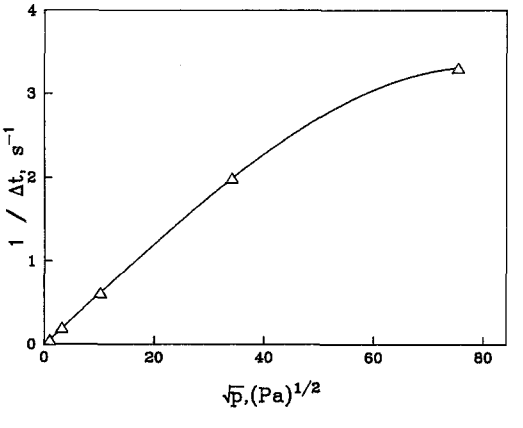

FIG. 7. Linear dependency of $(\Delta t)^{-1}$ on square root of initial ethylene pressure.

Other than the IR bands already mentioned, measureable changes in other bands could not be detected during this work. Changes in the populations of hydroxyl groups (3478 cm^{-1}) appeared only after the absorbances of the 1446-cm^{-1} band were large or after catalyst pretreatment at lower temperatures (700°C), supposedly retaining higher silanol populations.

DISCUSSION

Band Assignments

The earlier stated assignments of the stronger 2920- and 2850-cm^{-1} bands to polyethylene groups are evident (*14*). They grow together, change with reaction time, and are unaffected by evacuation of the IR cell. The band at 1472 cm^{-1} behaves somewhat similarly, but the experimental data suggest that it does not exhibit an induction period and does diminish somewhat upon evacuation of the cell. The residual absorbance after evacuation beyond roughly 2 s of polymerization may be related to overlap of the 1446-cm^{-1} band. Essentially, the three bands other than the 1446-cm^{-1} one relate to polyethylene methylene groups.

The 1446-cm^{-1} band may be assigned to weakly adsorbed ethylene on or in the vicinity of active (reduced) Cr atoms on the following basis:

(1) The bonding mode of gaseous ethylene differs by 2 cm^{-1} (Fig. 1).

(2) Gaseous ethylene exhibits much stronger absorbance in the bending rather than the stretching region (*21*). This may explain the inability to observe stretching bands for the adsorbed ethylene in this work.

(3) The two characteristic wings on each side of the central band at 1444 cm^{-1} for gaseous ethylene attributed to rotational

plus bending modes, disappear in the adsorbed state (1446-cm^{-1} band). Surface stabilization of the adsorbed species likely causes this loss of freedom.

(4) The total disappearance of this band upon early evacuation, whereas it partially disappears after some polymerization followed by evacuation, suggests that the polymer helps to confine some ethylene within the polymer mass.

(5) The absence of adsorption of ethylene observed on oxidized Cr/SiO_2 but the "adsorption isotherm" behaviour exhibited with reduced catalyst clearly suggests that the 1446-cm^{-1} band should be related to reduced Cr centers.

(6) The adsorption behaviour shown in Fig. 5 resembles that of a classical Langmuir isotherm (even though the data may not represent true equilibrium adsorption). Comparison of the number of Cr atoms with the amount of ethylene molecules "removeable" from the flat part of the "isotherm" shows a ratio of 0.28 ethylenes per Cr atom. Certain Cr atoms apparently stabilize adsorption of ethylene molecules in their vicinity, perhaps facilitating hydrogen-bonding type interactions between ethylenes and oxide ions in the support.

(7) The gradual increase in absorbance of the 1446-cm^{-1} band with polymerization time is attributed to overlap from the nearby 1472-cm^{-1} band whose intensity is increasing with time.

Rate Behaviour

The experimentally determined initial rates of reaction were obtained at near room temperature and rather low pressures of ethylene. A 0.78 order of reaction with respect to ethylene was observed in contrast to the frequently reported first order behaviour (often at higher temperatures and pressures). This suggests that the rate of reaction is mildly inhibited in some way. The linearity of the absorbance plots shown in Figs. 2 and 4, which characterize the data used to determine the 0.78 order, provides some confidence in this calculated order.

The induction period, labelled $\Delta(t)$ herein, which was observed between introduction of ethylene and the start of the polymerization reaction, is not related to catalyst activation since the experiments started with previously activated catalyst. The adsorbance–time plots show that ethylene initially adsorbs at a finite rate and during the latter stage of the initial adsorption kinetics, polymerization commences. Presumably, a build-up of surface concentration of ethylene is required before the reaction initiation process commences. This time delay was found to be inversely proportional to the square root of the initial pressure of ethylene as shown in the plot of Fig. 7. Figure 7 may be regarded as a plot of the adsorption rate function since $[\Delta(t)]^{-1}$ is somewhat proportional to the initial rate of adsorption. The square-root dependency of ethylene suggests that ethylene dissociates during adsorption on the reduced Cr sites. Such a buildup of surface carbene groups may occur on the more active sites but with limitations on their population, e.g., geometrical (adjacent pairs of active Cr sites needed) and high reactivity (short-lived intermediate), causing the time delay. This dissociative adsorption explanation coincides with the results recently published by Rebenstorf (*12*, *13*). On the basis of low-temperature CO adsorption experiments, Rebenstorf suggested that dinuclear species are the active forms involved in the polymerization at room temperature. On the other hand, Krauss used ethylene dissociation as a means of producing surface carbenes (*7*).

Additional support for a dissociative mechanism comes from the need for surface carbenes as a necessary byproduct involved in certain reactions observed on $Cr–SiO_2$ type catalysts (*7*, *23*, *24*) and as a surface species in this reaction system (*22*). The disappearance of some specific hydroxyl groups at the onset of polymerization reported earlier (*4*) is likely related to the process of adsorption of ethylene when ethylene first contacts the catalyst. The steps subsequent to initiation, e.g. propagation,

as proposed earlier (*4*), are not affected by this dissociative adsorption view.

Mechanism of Polymerization Initiation

Assuming that dissociation is the initial step in the reaction sequence, the dissociation could proceed in two ways:

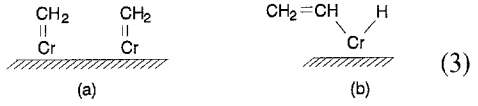

(3)

Considering the first possibility, the carbenes could act as a pair in initiating polymerization,

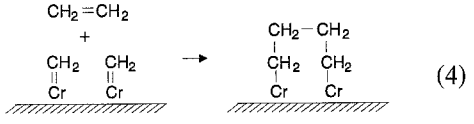

(4)

or as single sites, via either

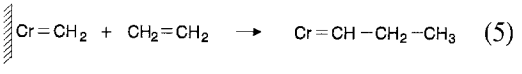

(5)

or

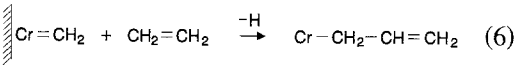

(6)

In the FTIR spectral scans recorded at the outset of the reaction, bands characteristic of methyl or vinyl groups were not detected supporting the view that they are not present in the reaction initiation. On the other hand, experiments using propylene or 1-hexene, which contain methyl groups, on the same activated catalyst, clearly showed IR evidence of methyl groups being present arguing that methyl groups if present during the polymerization of ethylene should be detectable. Although carbene groups also were not detected in the IR spectra, their participation as a short-lived intermediate species formed in the initiation step could explain their absence. Equation (4) appears to be the view appropriate for the experimental observations. The lack of observed vibrations for such terminal groups during early polymerization (*9*, *22*) even when the chain length was estimated to contain four carbons (*14*), with methylene vibrations being easily detectable, argues for the dissociation mechanism, Eqs. (3a) and (4). Also, step (4) involves only methylene groups, the only ones observed.

Propagation via Eq. (5) could involve carbene (*22*, *25*), or a carbane (*11*) mechanism without scrambling (*8*), on both Cr atoms involved. The metallacyclic mechanism on dinuclear Cr sites proposed recently (*9*) may also be valid in light of the above results; however, the 2750-cm^{-1} band, which should be observed relatively more easily early in the reaction, was not observed in the FTIR spectra.

CONCLUSIONS

1. Fast-scanning FTIR spectrometry enabled tracking of the interaction between ethylene and activated Cr/SiO_2 surface at room temperature from their first contacting through initiation and propagation of polymerization.

2. Ethylene adsorbs in molecular form reversibly and, also, dissociatively likely to form a reaction intermediate in the form of paired carbene structures linked to two Cr active sites. The absence of IR evidence suggests that the dissociation (initiation step) does not involve a hydrogen-donor component or the formation of methyl groups.

3. Adsorption and polymerization of ethylene on pre-activated catalyst are separated by a timelag, which is ethylene pressure-dependent. It is possible that the delay may be attributed to the kinetics of dissociation of molecularly adsorbed ethylene.

4. Polymerization of ethylene by addition of a monomer unit to a pair of carbenes results in a polymer chain linked at both ends to two active Cr sites. Subsequent insertions of monomer, i.e., propagation, are consistent with earlier mechanistic views.

ACKNOWLEDGMENTS

Financial support from NOVACOR, Ltd., and from the Natural Sciences and Engineering Research Council is gratefully acknowledged. The authors especially thank the reviewers for their very helpful comments.

REFERENCES

1. McDaniel, M. P., *Adv. Catal.* **33,** 47 (1985).
2. Hogan, J. P., *in* "Applied Industrial Catalysis," Vol. 1, chap. 6. Academic Press, New York, 1983.
3. McDaniel, M. P., Leigh, C. H., and Sharry, S. M., *J. Catal.* **120,** 170 (1989).
4. Jozwiak, W. K., Dalla Lana, I. G., and Fiedorow, R., *J. Catal.* **121,** 183 (1990).
5. Groeneveld, C., Wittgen, P. P. P. M. M., Swinnen, H. P. M., Wernsen, A., and Schuit, G. G., *J. Catal.* **83,** 346 (1983); **83,** 77 (1983).
6. McDaniel, M. P., and Welch, M. B., *J. Catal.* **82,** 98 (1983).
7. Krauss, H. L., and Hums, E., *Z. Naturforsch., B.: Anorg. Chem., Org. Chem.* **34b,** 1628 (1979).
8. McDaniel, M. P., and Cantor, D. M., *J. Polym. Sci., Polym. Chem. Ed.* **21,** 1217 (1983).
9. Chiotti, G., Garrone, E., and Zecchina, A., *J. Mol. Catal.* **46,** 61 (1988).
10. Rebenstorf, B., and Larsson, R., *J. Mol. Catal.* **11,** 247 (1981).
11. Rebenstorf, B., *Z. Anorg. Allg. Chem.* **513,** 103 (1984).
12. Rebenstorf, B., *Acta Chem. Scand.* **43,** 413 (1989).
13. Rebenstorf, B., *J. Catal.* **117,** 71 (1989).
14. Rebenstorf, B., *J. Mol. Catal.* **45,** 263 (1988).
15. Rebenstorf, B., *Z. Anorg. Allg. Chem.* **571,** 148 (1989).
16. Jozwiak, W. K., and Dalla Lana, I. G., paper in preparation.
17. Myers, D. L., and Lunsford, J. H., *J. Catal.* **92,** 260 (1985).
18. Myers, D. L., and Lunsford, J. H., *J. Catal.* **99,** 140 (1986).
19. Lunsford, J. H., Fu, S., and Myers, D. L., *J. Catal.* **111,** 231 (1988).
20. Karge, H. G., *Z. Phys. Chem.* **122,** 1033 (1980).
21. Pouchert, Ch. J., "The Aldrich Library of FT-IR Spectra-Vapor Phase," 1st ed., Vol. 3, Aldrich Chemical Co., Inc., Milwaukee, Wisconsin, 1989.
22. Chiotti, G., Garrone, E. Coluccia, C., Morterra, C., and Zecchina, A., *J. Chem. Soc. Chem. Commun.* **801,** 1032, (1979).
23. Krauss, H. L., and Hums, E., *Z. Naturforsch., B: Anorg. Chem., Org. Chem.* **35b,** 848 (1980).
24. Krauss, H. L., and Hums, E., *Z. Naturforsch., B: Anorg. Chem., Org. Chem.* **38b,** 1412 (1983).
25. K. J. Ivin, Rooney, J. J., Stewart, C. D., Green, M. L. H., and Mahtab, R., *J. Chem. Soc. Chem. Commun.* **Com. 323,** 604 (1978).